

IMPROVING CHARACTERISTICS OF NANOSTRUCTURED DEVICES BY SEPARATE CONFINEMENT HETEROSTRUCTURE LAYER

G. Sh. Shmavonyan

*Microelectronic and Biomedical Devices Department, State Engineering University of Armenia,
Yerevan, Armenia, e-mail: gshmavon@yahoo.com*

Received 25 May, 2011

Abstract—Experiments show that the layer of separate confinement heterostructure (SCH) has a significant influence on the emission spectrum of semiconductor optical amplifiers (SOAs). Reducing the thickness of the SCH layer at the p-side could improve the uniformity of carrier distribution among multiple quantum wells (MQWs). With three $\text{In}_{0.67}\text{Ga}_{0.33}\text{As}_{0.72}\text{P}_{0.28}$ QWs near the p-side and two $\text{In}_{0.53}\text{Ga}_{0.47}\text{As}$ QWs near the n-side, when the thickness of the SCH layer changes from 120 nm to 30 nm, the operation current for SOAs to exhibit the full-width at half-maximum (FWHM) spectral width of above 270 nm could be reduced from 500 mA to 160 mA.

Keywords: separate confinement heterostructure layer, carrier distribution, multiple quantum wells, nanostructured devices, operation current.

1. Introduction

The optical fiber for optical communication exhibits very low loss between 1.3 and 1.6 μm , so the optical components used in the fiber-optic communications are expected to cover the same broad bandwidth. Unfortunately, the light sources and optical amplifiers, e.g., the Er-doped fiber amplifiers/lasers and conventional semiconductor optical amplifiers (SOAs), are usually only available with a relatively narrow bandwidth. Therefore, schemes for broadening their bandwidth are very attractive. A single quantum well (QW) with simultaneous transitions of $n = 1$ and $n = 2$ states [1, 2] and non-identical multiple quantum wells (MQW) [3-6] had been used to broaden the SOA bandwidth. The latter approach is particularly attractive because the spectral width is less influenced by the device length [4–7]. However, the MQW structure exhibits non-uniform carrier distribution [8-11], which significantly influences the broad-band characteristics of the SOA [12, 13]. The non-uniform carrier distribution has been found to be influenced by the height and the thickness of the barriers [14, 15] and the sequence of the MQW layout [12]. Here we report the strong influence of the separate confinement heterostructure (SCH) layer on the carrier distribution among MQWs, the emission spectrum and operation current of the SOA.

2. Experiment

Three QW structures with different SCH layers were experimented. As shown in Fig. 1, the QW structures consist of three 6 nm $\text{In}_{0.67}\text{Ga}_{0.33}\text{As}_{0.72}\text{P}_{0.28}$ QWs and two 15 nm $\text{In}_{0.53}\text{Ga}_{0.47}\text{As}$ QWs with their first quantized energies corresponding to 1.3 μm and 1.6 μm , respectively. The QWs are separated by 15 nm $\text{In}_{0.86}\text{Ga}_{0.14}\text{As}_{0.3}\text{P}_{0.7}$ barriers. Samples A and B have 120 nm and 80 nm SCH layers, respectively. The thickness of the SCH layers for sample C is 30 nm at the p-side and 120

nm at the n-side. The SCH layers, barriers, and QWs are not doped. They are sandwiched between the InP p-cladding layer and the InP n-cladding layer. The p-cladding layer is Zn-doped with measured concentration $p > 10^{18}/\text{cm}^3$. Above the p-cladding layer, there is an $\text{In}_x\text{Ga}_{1-x}\text{As}$ cap layer with measured concentration $p > 2 \times 10^{19}/\text{cm}^3$. The n-cladding layer is also epitaxially grown with $n = 1 \times 10^{18} \text{ cm}^{-3}$ for 0.5 μm and with $n = 5 \times 10^{18} \text{ cm}^{-3}$ for another 0.5 μm .

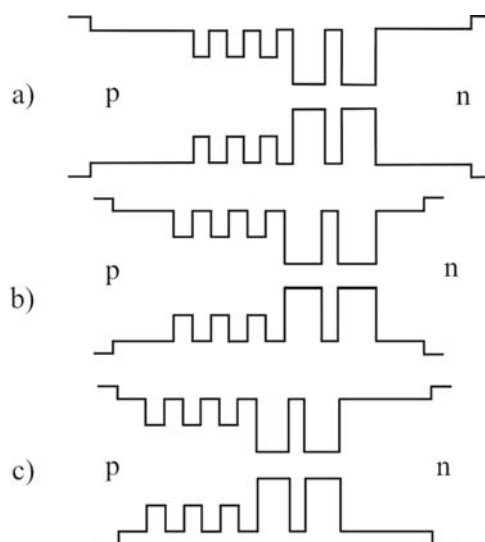


Fig. 1. QW structures of SOA used in the experiment. Thicknesses of SCH layers for samples for p-side are a) sample A – 120 nm, b) sample B – 80 nm, c) sample C – 30 nm and for n-side – 120 nm. The barrier is $\text{In}_{0.86}\text{Ga}_{0.14}\text{As}_{0.3}\text{P}_{0.7}$ (15 nm); QWs are three 6 nm $\text{In}_{0.67}\text{Ga}_{0.33}\text{As}_{0.72}\text{P}_{0.28}$ and two 15 nm $\text{In}_{0.53}\text{Ga}_{0.47}\text{As}$.

SOAs were fabricated on those substrates using typical processing techniques. The devices had the 3 μm ridge waveguide tilted at 5° from the normal of the cleaved facet to reduce the Fabry-Perot resonance. In addition, the device length was made to be as short as 300 μm to minimize the amplified spontaneous emission (ASE). Thus, the emission spectrum could directly reflect the carrier distribution among the different types of QWs. No facet coatings were applied to the devices.

3. Results and Discussion

The measured emission spectra are shown in Fig. 2a-c. At the current of 20 mA, the emission spectra are around 1500-1600 nm for all samples. They are mainly contributed from the $\text{In}_{0.53}\text{Ga}_{0.47}\text{As}$ QWs. As the injection current increases, the spectra broaden toward the short-wavelength range due to the contribution first from the second quantization level of the $\text{In}_x\text{Ga}_{1-x}\text{As}$ QWs and then from the $\text{In}_x\text{Ga}_{1-x}\text{As}_y\text{P}_{1-y}$ QWs. This means that the injected carriers first get captured into the $\text{In}_x\text{Ga}_{1-x}\text{As}$ QWs. As the carrier density increases, some carriers are captured into the $\text{In}_x\text{Ga}_{1-x}\text{As}_y\text{P}_{1-y}$ QWs. However, for sample A, the contribution from the $\text{In}_x\text{Ga}_{1-x}\text{As}_y\text{P}_{1-y}$ QWs is observed only when the injection current is near 500 mA. In comparison, samples B and C have

their emission contributed from the $\text{In}_x\text{Ga}_{1-x}\text{As}_y\text{P}_{1-y}$ QWs at a much lower injection current. For sample C, the contribution from the $\text{In}_x\text{Ga}_{1-x}\text{As}_y\text{P}_{1-y}$ QWs already appears at the injection current of 160 mA. This indicates that sample B and sample C have the carriers captured into the $\text{In}_x\text{Ga}_{1-x}\text{As}_y\text{P}_{1-y}$ QWs before the $\text{In}_x\text{Ga}_{1-x}\text{As}$ QWs are filled up. The above emission spectra clearly show that the thickness of the SCH layer has a significant influence on the emission spectrum of the SOAs with non-identical MQWs.

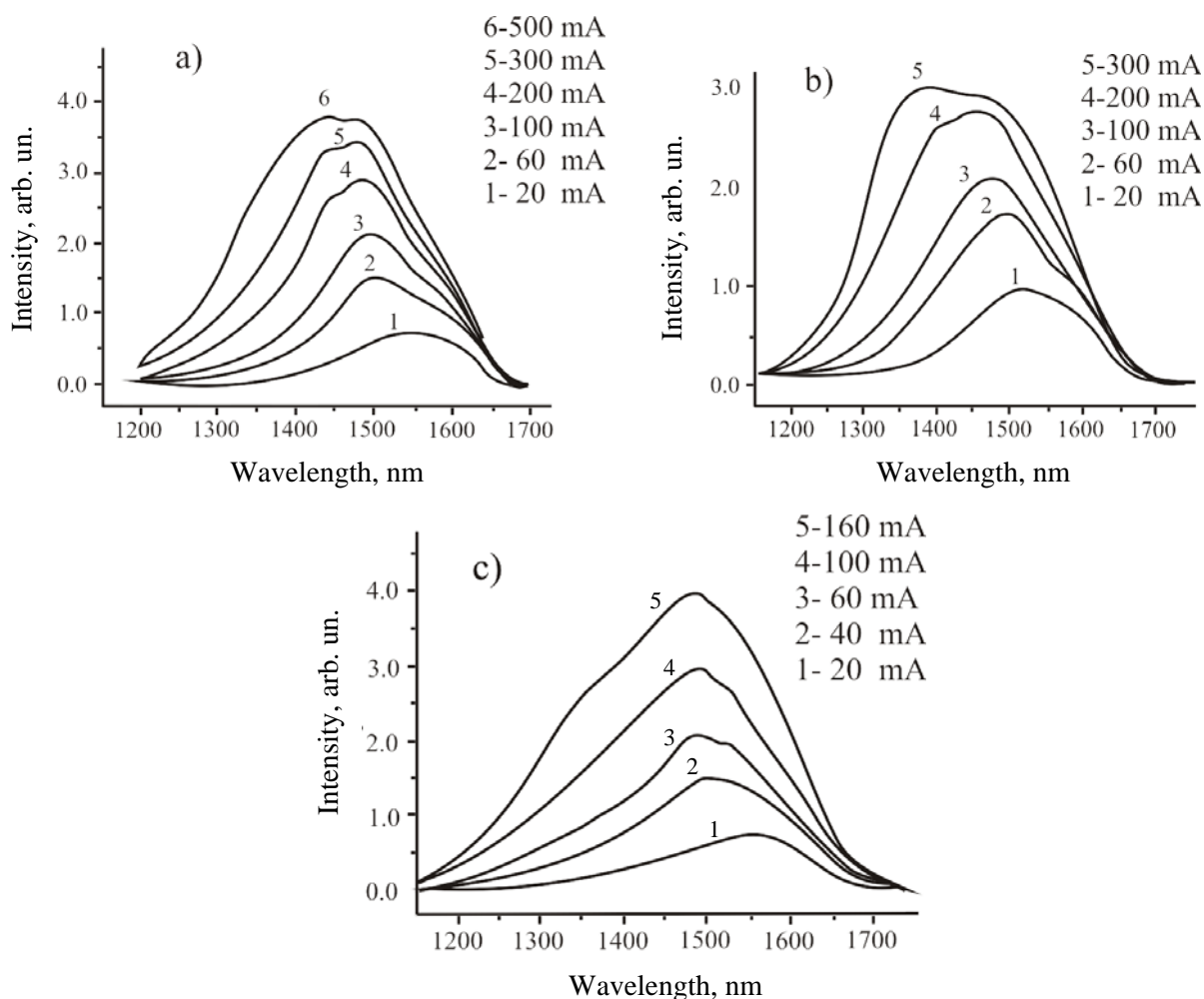


Fig. 2. Emission spectra of SOA at different levels of injection current: a) sample A, b) sample B, c) sample C.

The FWHM of the emission spectrum versus the injection current is shown in Fig. 3. At the low injection current, their FWHM widths are about the same. For sample A, the FWHM increases slowly with the injection current. For sample B, the FWHM spectral width increases much faster than sample A. For sample C, the FWHM spectral width increases even faster than sample B. At the injection current of 160 mA, sample C has the FWHM of the emission covering from 1310 to 1600 nm. This FWHM spectral width is even larger than that of sample A at the high injection current of 500 mA.

Because the corresponding wavelengths of the two types of QWs are very different, the measured spectrum could help identify the contribution from each type of the QWs and reflect the

carrier distribution among the MQWs. The measured spectra and the FWHM spectral width reveal that the carrier distribution among the MQWs in the three samples is not the same. For sample A, carrier distribution favors the $\text{In}_x\text{Ga}_{1-x}\text{As}$ QWs near the n-cladding for most of the injection current levels due to the electron determined non-uniform carrier distribution [13] as a result of the thick SCH layer. In sample B, the reduced SCH thickness causes holes to arrive at the QW region sooner than in sample A. The preference of the carrier distribution in the QWs near the n-side is reduced, so carriers can distribute among the QWs near the p-side at a lower injection current. For sample C, the SCH thickness is further reduced to only 30 nm at the p-side. The transport time of holes to the QWs is then significantly reduced, so carriers are able to distribute in the QWs at the p-side at a much lower injection current. This leads to better uniformity of carrier distribution among the QWs and results in a very broad emission spectrum at a low current density. Therefore, to obtain the bandwidth of 260 nm, the operation current is only 200 and 100 mA for sample B and sample C, respectively, but is near 500 mA for sample A. It shows that the transport time of holes across the SCH layer is an important factor influencing the carrier distribution among MQWs.

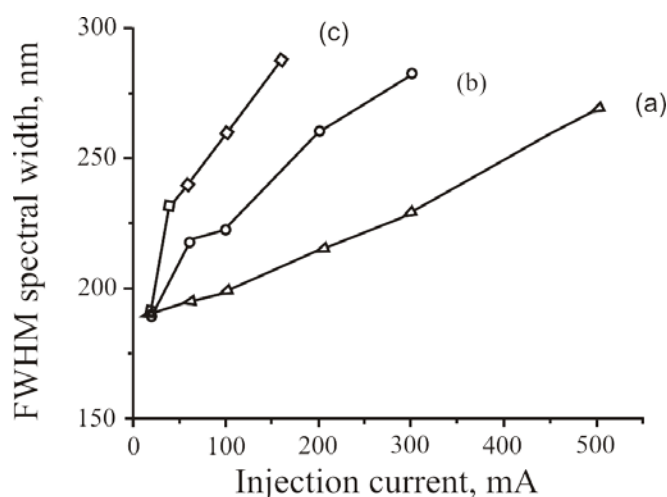


Fig. 3. Variation of FWHM spectral width with injection current: a) sample A, b) sample B, c) sample C.

The narrow SCH layer may cause the doped Zn to diffuse into the $\text{In}_{0.67}\text{Ga}_{0.33}\text{As}_{0.72}\text{P}_{0.28}$ QWs that are near the p-side. If this happens, the emission contributed from these QWs should decrease. Because these QWs correspond to the short wavelength, samples B and C then should have less emission at short wavelengths and, hence, narrower spectral width than sample A. However, our experiments show the opposite behavior, so the Zn diffusion into the QWs is negligible.

With non-identical MQWs, the light at the short wavelength may be absorbed by the QWs corresponding to the long wavelength, so the measured emission spectra at the low injection current only appear at the long wavelength for all samples. Such a factor causes the long wavelength QWs to accumulate more carriers than short wavelength QWs. Therefore, we use more 6 nm $\text{In}_{0.67}\text{Ga}_{0.33}\text{As}_{0.72}\text{P}_{0.28}$ QWs than 15 nm $\text{In}_{0.53}\text{Ga}_{0.47}\text{As}$ QWs to compensate for such an effect.

Because this factor is the same for all of the three samples, it is not the reason for the difference in their spectral behaviors.

The measured output power (L) and voltage (V) versus current (I) are shown in Fig. 4. The I - V curve shows that the SCH thickness has no influence on the turn-ON voltage, which is slightly less than 1 V, almost identical for all samples. The output power is low for all of the three samples because the broad bandwidth reduces the ASE level [16]. Sample C has the broadest bandwidth, so it has the lowest power. The L - I curve has a decreasing slope because of the increased temperature at the large injection current. The L - I curve of the 300 μm Fabry-Perot laser diode (LD) fabricated on sample B is also plotted on the same figure for comparison. This LD has the threshold current around 100 mA. Its L - I curve also has a decreasing slope before lasing.

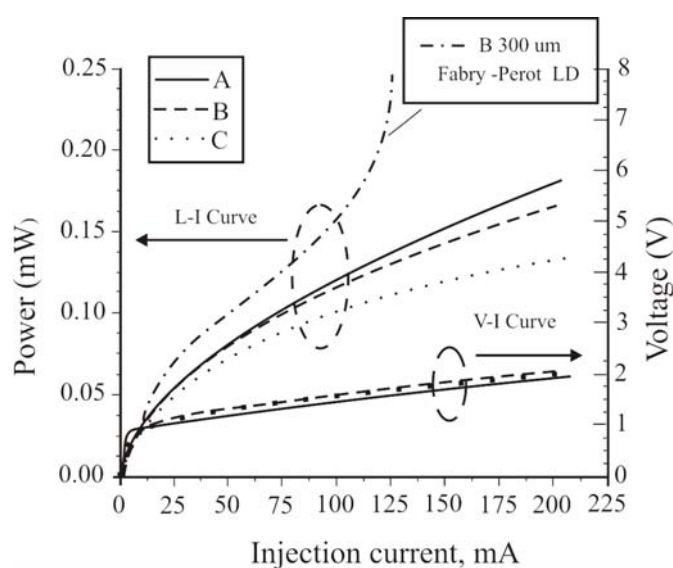


Fig. 4. Measured L - V - I . (Solid line: sample A. Dashed line: sample B. Dotted line: sample C). The L - I curve of a Fabry-Perot LD with threshold current ~ 100 mA is also shown for comparison.

Thus, the influence of the SCH layer on the field distribution has also been evaluated. As the SCH thickness reduces, the near field slightly expands vertically and so the vertical far-field angle decreases. The measured vertical angles (FWHM) of the far field are 50° , 48° , and 47° , respectively, for the Fabry-Perot LDs made on samples A, B, and C. The expanded near field in sample C would slightly increase the loss due to free carrier absorption in the cladding layers.

4. Conclusion

The SCH layer is found to have a significant influence on the carrier distribution among the non-identical MQWS and the emission spectrum of SOAs. With the 120 nm SCH layer, the SOAs have the FWHM spectral width of about 270 nm at the 500 mA of injection current. As the SCH layer at the p-side is reduced to 30 nm, the FWHM spectral increases to 290 nm at the low injection current of 160 mA.

REFERENCES

1. **A.T.Semenov, V.R.Shidlovski, S.A.Safin**, Electron. Lett., **29**, 854 (1993).
2. **T.R.Chen, L.Eng, Y.H.Zhuang, A.Yariv**, Appl. Phys. Lett., **56**, 1345 (1990).
3. **C.-F.Lin, B.-L.Lee, B.-J.Lin**, IEEE Photon. Technol. Lett., **8**, 1456 (1996).
4. **X.Zhu, D.Cassidy, M.Hamp, D.Thompson, B.Robinson, Q.Zhao, M.Davies**, IEEE Photon. Technol. Lett., **9**, 1202 (1997).
5. **H.S.Gingrich, D.R.Chumney, S.-Z.Sun, S.D.Hersee, L.F.Lester, S.R.Brueck**, IEEE Photon. Technol. Lett., **9**, 155 (1997).
6. **C.-F.Lin, B.-L.Lee**, Appl. Phys. Lett., **71**, 1598 (1997).
7. **T.F.Krauss, G.Hondromitros, B.Vogele, R.M.De La Rue**, Electron. Lett., **33**, 1142 (1997).
8. **N.Tessler, G.Eisenstein**, IEEE J. Quantum Electron., **29**, 1586 (1993).
9. **R.Nagarajan, T.Fukushima, S.W.Corzine, J.E.Bowers**, Appl. Phys. Lett., **59**, 1835 (1991).
10. **H.Yamazaki, A.Tomita, M.Yamaguchi, Y.Sasaki**, Appl. Phys. Lett., **71**, 767 (1997).
11. **B.-L.Lee, C.-F.Lin, L.-W.Laih, W.Lin**, Electron. Lett., **34**, 1230 (1998).
12. **C.-F.Lin, B.-R.Wu, L.-W.Laih, T.-T.Shih**, Opt. Lett., **26**, 1099 (2001).
13. **C.-F.Lin, B.-R.Wu, L.-W.Laih**, J. Appl. Phys., **42**, 5557 (2003).
14. **M.J.Hamp, D.T.Cassidy, B.J.Robinson, Q.C.Zhao, D.A.Thompson, M.Davies**, IEEE Photon. Technol. Lett., **10**, 1380 (1998).
15. **M.J.Hamp, D.T.Cassidy, B.J.Robinson, Q.C.Zhao, D.A.Thompson**, IEEE Photon. Technol. Lett., **12**, 134 (2000).
16. **C.-F.Lin, Y.-S.Su, B.-R.Wu**, IEEE Photon. Technol. Lett., **14**, 3 (2002).